AD-A038 497 PURDUE UNIV LAFAYETTE IND F/G 8/2
PHOTOGRAMMETRIC ASPECTS OF THE HETERODYNE OPTICAL CORRELATOR.(U)
JUL 76 E M MIKHAIL DAAGZ9-76-D-0100
UNCLASSIFIED ETL-0095 NL

| OF |
AD
A038497

END

DATE
FILMED
5-77

ETL - 0095

ADA038497

12 NW

PHOTOGRAMMETRIC ASPECTS OF THE HETERODYNE OPTICAL CORRELATOR

JULY 1976

DDC RECEIVED APR 21 1977 C

AD NO. DDC FILE COPY

Approved for public release; Distribution unlimited.

U.S. ARMY ENGINEER
TOPOGRAPHIC LABORATORIES
FORT BELVOIR, VA 22060

Destroy this report when no longer needed.
Do not return it to the originator.

The findings in this report are not to be construed as an official Department of the Army position unless so designated by other authorized documents.

The citation in this report of trade names of commercially available products does not constitute official endorsement or approval of the use of such products.

UNCLASSIFIED

SECURITY CLASSIFICATION OF THIS PAGE *(When Data Entered)*

REPORT DOCUMENTATION PAGE		READ INSTRUCTIONS BEFORE COMPLETING FORM
1. REPORT NUMBER: ETL-0095	2. GOVT ACCESSION NO.	3. RECIPIENT'S CATALOG NUMBER
4. TITLE *(and Subtitle)*: PHOTOGRAMMETRIC ASPECTS OF THE HETERODYNE OPTICAL CORRELATOR		5. TYPE OF REPORT & PERIOD COVERED: Contract Report 6. PERFORMING ORG. REPORT NUMBER
7. AUTHOR(s): Edward M. Mikhail		8. CONTRACT OR GRANT NUMBER(s): DAAGZ9-76-D-0100 new
9. PERFORMING ORGANIZATION NAME AND ADDRESS: Purdue University, Lafayette, Indiana 47907		10. PROGRAM ELEMENT, PROJECT, TASK AREA & WORK UNIT NUMBERS: 50 p.
11. CONTROLLING OFFICE NAME AND ADDRESS: US Army Engineer Topographic Laboratories, Fort Belvoir, Virginia 22060		12. REPORT DATE: July 1976 13. NUMBER OF PAGES: 41
14. MONITORING AGENCY NAME & ADDRESS *(if different from Controlling Office)*		15. SECURITY CLASS. *(of this report)*: UNCLAS 15a. DECLASSIFICATION/DOWNGRADING SCHEDULE

16. DISTRIBUTION STATEMENT *(of this Report)*

Approved for public release; distribution unlimited.

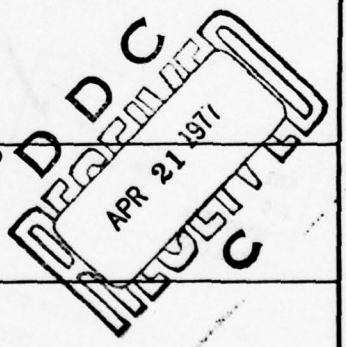

17. DISTRIBUTION STATEMENT *(of the abstract entered in Block 20, if different from Report)*

18. SUPPLEMENTARY NOTES

19. KEY WORDS *(Continue on reverse side if necessary and identify by block number)*

Coherent Optics
Optical Spatial Correlation
Photometric Data Extraction

20. ABSTRACT *(Continue on reverse side if necessary and identify by block number)*

Heterodyne optical correlation as applied to coherently illuminated overlapping transparencies is briefly discussed. Photogrammetric aspects of optical image coincidence are carefully studied for vertical as well as tilted photography. An experimental Heterodyne Optical Correlator (HOC) is described. A two-dimensional photo diode detector array is used in the output plane as a precise measuring system. It is shown that for regular aerial photography, it is not possible to place the transparencies untilted in the correlator and → OVER

DD FORM 1 JAN 73 1473 EDITION OF 1 NOV 65 IS OBSOLETE

UNCLASSIFIED 221 650

SECURITY CLASSIFICATION OF THIS PAGE (When Data Entered)

expect tolerable y-parallaxes. Therefore, either the transparencies must be tilted, or the HOC should operate essentially as a comparator, with correlation taking place in the image space. For the latter case, one transparency is fixed and the other is moved in steps in both the x- and y-directions. The result is that for each array element one gets x, y coordinates on one transparency and p_x, p_y parallaxes from the other.

The results of two preliminary tests using aerial photography are given. They indicate accuracies of about one to two parallax steps (one step = 25 μm in the tests). However, the tests are so limited that the results should be considered only as preliminary, indicating the feasibility of the system as an area correlator. Further development and more extensive testing are recommended before the potential and accuracy of the HOC system may be determined.

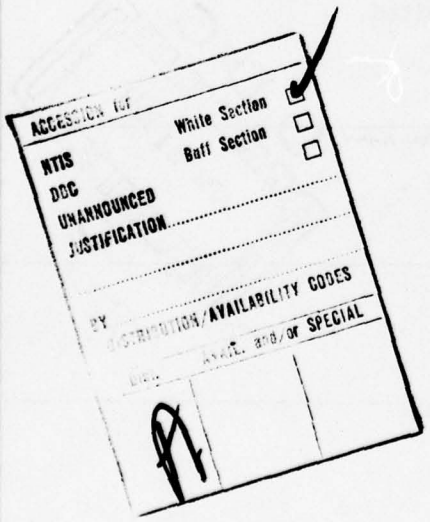

FOREWORD

The Center for Coherent Optics of the Research Institute, U.S. Army Engineer Topographic Laboratories (ETL), has been instrumental in advancing research and development in the application of coherent optical techniques to various mapping operations. In a continuing effort to investigate the potential of coherent optical heterodyne coincidence detection techniques, research support has been made available to Dr. N. Balasubramanian as an optical engineer and to the author as a photogrammetrist. This report summarizes earlier photogrammetric analyses and documents in detail data obtained using actual aerial photography on an experimental Heterodyne Optical Correlator (HOC). The theory and optical design considerations of the HOC system are given in a separate but allied report, No. ETL-0071, titled "Experimental Heterodyne Optical Correlator," by Dr. Balasubramanian (see reference (1)). It is advised that in order to attain complete grasp of the HOC system and its potential both reports should be read, since they are intended to compliment each other.

The author wishes to acknowledge Dr. Balasubramanian's cooperation and continuous support with regard to optical aspects. He also acknowledges the Commanding Director of ETL, Col. M. K. Kurtz, Jr.; Mr. R. P. Macchia, ETL's Technical Director; and Dr. A. Mancini, the Director of the Research Institute for their continued interest in and support of developments in coherent optics in mapping. Special thanks are due Dr. R. D. Leighty, Chief of the Center for Coherent Optics, for his

untiring efforts and unceasing encouragement during the course of the research leading to this report; and to the following members of ETL who provided assistance in various forms: Mr. J. R. Benton, Dr. W. W. Seemuller, Mr. G. E. Lukes, Mr. R. S. Pazak and Mr. M. Roos.

TABLE OF CONTENTS

SUMMARY

This report discusses the photogrammetric aspects of the Heterodyne Optical Correlator (HOC) which is based on coherent optical techniques. Various photogrammetric considerations both for the manner in which the overlapping transparencies are introduced in HOC, and the mode of its operation for photogrammetric data extraction, are analyzed. An experimental HOC system, built in the optics laboratory mainly to demonstrate the conceptual feasibility of the correlator, is briefly described. Very preliminary test data from two small areas in two different photogrammetric models, comprised of overlapping aerial photographs, are given. In the tests, the transparencies are inserted in essentially the same plane and projected through the system such that their projections superimpose on a square detector array. The output from the HOC system is a square matrix of numbers, the same order as the detector array, which can be readily converted to image locations on one transparency and the corresponding parallax values on the other. The results obtained indicate the feasibility of HOC as an area correlator capable of parallel processing of a large number of elemental areas (1024 in the experimental model) on overlapping imagery. It is important to emphasize, however, that both the experimental system and the tests are preliminary in nature and are intended for providing background information to guide future development.

LIST OF FIGURES

LIST OF TABLES

CHAPTER 1

INTRODUCTION

The Heterodyne Optical Correlator (HOC) is a system for image correlation which is based on the principle of heterodyne optical coincidence detection (1, 2). Unlike electronic correlators which convert image information to electrical signals and perform correlation in the time domain, the HOC achieves correlation in the space domain. The two transparencies which form a stereo-pair are coherently illuminated and optically projected onto a common image (output) plane where the coincidence is detected. Using heterodyne optical techniques a normalized correlation coefficient value is obtained at each element of a photo diode array detector located in the output image plane. The heterodyne principle is implemented in the Mach-Zehnder interferometer of Figure 1 by moving mirror M_2 in a periodic manner. The normalized correlation coefficient at a point P in the output plane is given by

$$C_{12}(x_0, y_0; P) = \frac{\iint_A t_1(x, y)\, t_2(x+x_0, y+y_0)\, dA}{\left[\iint_A |t_1(x, y)|^2 dA \iint_A |t_2(x+x_0, y+y_0)|^2 dA\right]^{\frac{1}{2}}} \qquad (1)$$

where:

t_1 and t_2 are the amplitude transmittances for the two transparencies

x_0, y_0 are the relative displacements in the x- and y-directions, respectively, between the two transparencies

A is the area of a detector array element (over which matching is effected).

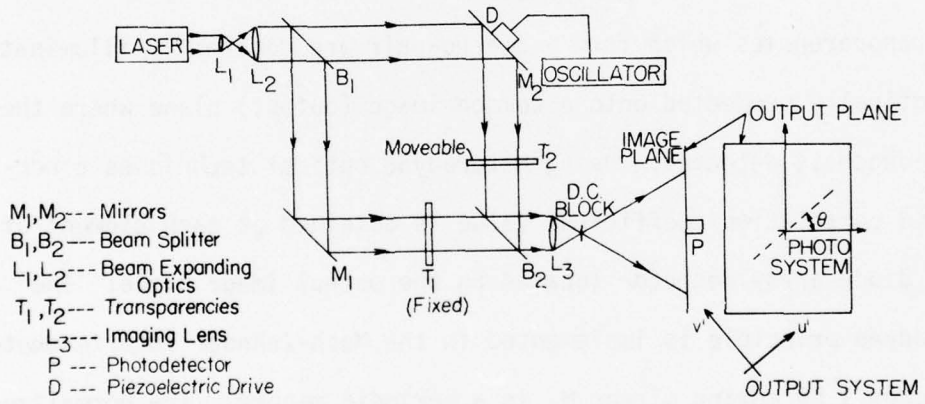

Figure 1. Mach-Zehnder Interferometric Arrangement.

Normalization in the function of equation (1) is possible through making two additional measurements besides the a.c. signal obtained when the two transparencies are simultaneously illuminated (the numerator in equation (1)). These measurements are the two d.c. signals (shown in the denominator of equation (1)) obtained when each transparency is illuminated alone.

Optical heterodyne detection may be applied to different systems. In this report consideration is limited to the experimental system depicted in Figure 2 and used for the extraction of terrain digital data from overlapping photographs. Furthermore, only photogrammetric aspects will be discussed since the theory and optical considerations on which the HOC is built are given in detail in reference (1). The main objectives are to discuss the basic photogrammetric factors involved in heterodyne optical correlation, describe an experimental HOC system, and present and analyze some preliminary test data obtained from the experimental system.

In Chapter 2 the general photogrammetric aspects of image coincidence in an optical correlator are reviewed. It begins with the relatively uninvolved case of truly vertical photography and ends with the general case of tilted aerial photography and its relation to the vertical case. In Chapter 3, the experimental HOC system of Figure 2 is first described and its characteristics enumerated. This is followed by an investigative study of the effect of untilting the transparencies in the HOC. Other sections discuss the operational mode of the experimental HOC and the procedure for computing ground coordinates from its data. Chapter 3 ends with some preliminary data obtained

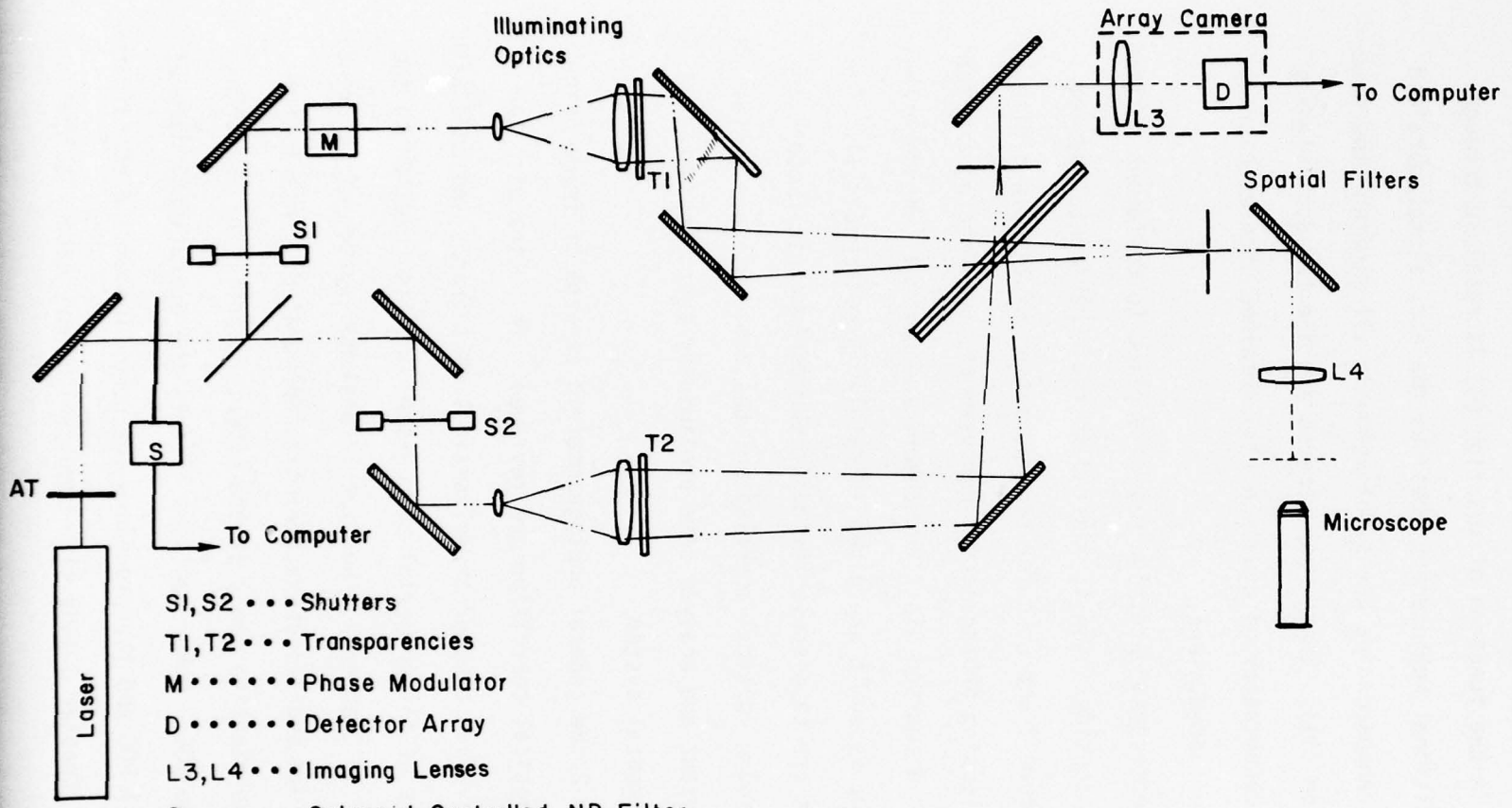

Figure 2. Experimental HOC System.

using overlapping aerial frame photographs. The report is concluded, in Chapter 4, by some recommendations drawn on the basis of the limited and preliminary test data obtained.

CHAPTER 2

GENERAL PHOTOGRAMMETRIC ASPECTS OF IMAGE COINCIDENCE

2.1 Truly Vertical Photography

Assume that we have a pair of overlapping truly vertical aerial photographs of flat level terrain printed on transparent material. If these photographs are superimposed, the overlap imagery would match perfectly if we assume that image displacements due to systematic effects can be neglected. The reason for the match is that each photograph in this case represents a map, or a scaled orthographic projection of the object plane.

Let us now assume that, instead of being flat, the terrain contains relief. When the two transparencies are superimposed in the overlap area, only points which have the same elevation will coincide on each other. Points which are either higher or lower than the matched points will exhibit separation in the x-direction, or the direction of the base between the two photographs. Such separation has been termed x-parallax differences, or Δp_x. Therefore in order to bring points at a different elevation level (i.e. contour) one transparency needs to be shifted in only the x-direction by an amount Δx given by [2]

$$\Delta x_{i,i+1} = \frac{Bf(Z_{i+1} - Z_i)}{(Z_c - Z_i)(Z_c - Z_{i+1})} \qquad (2)$$

where

$\Delta x_{i,i+1}$ is the shift in the plane of the transparencies to bring points of elevation Z_{i+1} in coincidence after matching the points at elevation Z_i

f is the focal length of the photography; both f and Δx have the same units

B is the value of the air-base in object space units

Z_c the flying height above datum, of both transparencies.

If the transparencies have been either magnified or reduced from the original format by a factor k, then the shift will be $k\Delta x_{i,i+1}$.

The case discussed above applies equally to the situation where the base has two components B_X and B_Y (but not B_Z and still strictly vertical photography) by using $B = (B_X^2 + B_Y^2)^{\frac{1}{2}}$ in equation (2). Here, the total base B is used and the shift is effected in the direction of the total base and not in the direction of the x-axis. Alternatively, two component shifts Δx using B_X (instead of B in equation (2)) and Δy using B_Y may be used.

The presence of B_Z (in strictly vertical photography) changes the situation somewhat. It is now not possible to match points of equal elevation by superimposing one transparency over the other because each set of equal elevation points are imaged at a slightly different scale on each transparency. Consequently, we modify the concept and think of projecting each transparency at a different scale onto a common (output) plane, such as the image plane in Figure 1 and the plane of the detector array D in Figure 2. Once those points at elevation Z_i are matched, one transparency needs to be shifted in the x- and y-

directions and its magnification changed before points with elevation Z_{i+1} are brought to coincide at the output plane. The values of the shifts and magnification change are given by:

$$\Delta x_{i,i+1} = \frac{k\, B_X\, f(Z_{i+1} - Z_i)}{(Z_c - Z_i)(Z_c + B_Z - Z_{i+1})} \tag{3a}$$

$$\Delta y_{i,i+1} = \frac{k\, B_y\, f(Z_{i+1} - Z_i)}{(Z_c - Z_i)(Z_c + B_Z - Z_{i+1})} \tag{3b}$$

$$m_{i,i+1} = \frac{(Z_c - Z_{i+1})(Z_c + B_Z - Z_i)}{(Z_c - Z_i)(Z_c + B_Z - Z_{i+1})} \tag{3c}$$

where:

- k is the scale factor between the fixed transparency and the output plane,
- B_X, B_Y, B_Z are the air-base components in the object space units,
- f the camera focal length
- Z_c the flying height above datum of the fixed transparency.

In all the cases discussed so far the output plane is parallel to the plane of the transparencies. The two-dimensional coordinates (x_i, y_i) of every set of matched points (at elevation Z_i, or on contour Z_i) are related directly to image coordinates. Therefore, if all (x_i, y_i) are multiplied by the corresponding scale for Z_i, we will get the corresponding horizontal coordinates in the object space (taking the horizontal position of the exposure station for the fixed transparency into account).

2.2 Tilted Photography

The cases discussed in the preceding section are characterized by having the camera axes normal to the datum. Therefore, they are

applicable to situations where the camera orientation can be controlled, as for example in close-range and terrestrial applications, or when the aerial photographs are rectified. If the available aerial photography is to be used directly in the HOC without rectification, then the transparencies may be tilted relative to the output plane. Since the digital data extracted from the correlator require further processing to convert it to a map system, it is advantageous to place one transparency parallel to the output plane. The second transparency will then accommodate the total relative tilt in the model.

Let M_1 and M_2 represent the orientation matrices of the two transparencies with respect to the object space coordinate system. If the first transparency is placed in the correlator parallel to the output plane, its matrix becomes the identity matrix. The relative orientation matrix for the second transparency becomes $R = M_2 M_1^t$ with respect to both the first transparency and the output plane. This means that the matrix R rotates the coordinate system of the output plane into the system of coordinates of the second (tilted) transparency. Three sequential angles may be derived from R according to the design of the holder used for the second transparency. Both the sense (or sign) of the rotation angles as well as their sequence are important in this computation. Once computed, the three angles must be introduced into the holder of the second transparancy in the proper sequence.

When the two transparencies are properly oriented in the HOC, the two images projected on the output plane will represent two photographs taken with the camera axes normal to the reference plane. Consequently, to proceed from a set of matched points on one contour to another set

on a different contour, it has been shown [2] that one needs to shift one transparency in the x- and y- directions and effect a change in scale. While it is possible in principle to manipulate either transparency, it is more convenient to move the transparency that is parallel to the reference output plane. This has a two-fold advantage: the first is that the shifts are in a plane parallel to the reference plane and thus related to it by a scale factor, and the second is that the relations derived for the truly vertical case apply equally here. Therefore, the three equations (3a), (3b), and (3c) are used to effect the matching of points on the (i+1) 'contour' line after those on the ith 'contour' line have been matched. The word 'contour' is not used here in the strict sense to mean points of equal elevation in the object space. Instead, it refers to points of equal elevation with respect to the output plane (which is parallel to the moveable photograph) as a model datum. Consequently, when a set of matched points are rotated into the object space system, although they will lie on one plane, that plane will not in general be parallel to the object datum plane. The rotation matrix is the same as the orientation matrix of the photograph that was placed parallel to the output plane in the HOC. The degree of tilt in that photograph will determine how far off is a set of matched points from falling on a contour line. In most cases the rotated points should be treated as an irregular digital terrain model from which contour lines may be interpolated using one of the many algorithms already derived for the purpose.

So far the basic scheme of data extraction has been to match a set of points in plane parallel to the reference output plane, then

compute shifts and scale change and introduce them in the HOC to effect coincidence of points in another plane. The coincidence is assumed on the basis of the fact that the value of the normalized cross-correlation coefficient exceeds a preselected threshold value. Therefore, the adequacy of the data extracted in this manner depends to a large extent on the suitability of the designated threshold value. If, for example, topography changes significantly from one area to another within a given model, the maximum value of the normalized cross-correlation coefficient is likely to be lower in areas of rugged terrain than in areas of relatively constant elevation. This is predominantly due to the existence of slope which causes localized changes in y-parallax and the consequent reduction in the value of the correlation coefficient. As a result, if only one threshold value is selected for the correlation coefficient, it is likely that it will not be adequate for all regions within the model. This fact was instrumental in devising another scheme for data extraction which allows for having varying values for the maximum correlation coefficient. This scheme is explained in detail in conjunction with the analysis of the experimental HOC system given in the following chapter.

CHAPTER 3

PHOTOGRAMMETRIC ANALYSIS OF THE EXPERIMENTAL HOC SYSTEM

3.1 Introduction

In the preceding two chapters we have given a broad account of heterodyne optical correlation and its general photogrammetric characteristics. Although it is likely that an engineering HOC model may be constructed on the basis of the general system described, when an experimental system was attempted in the laboratory a somewhat different HOC evolved. The difference is not only in the electro-optical components, but also in the photogrammetric data extraction scheme, and hence in the basic operational mode of the system. The following section describes in detail the experimental HOC system and its specification.

3.2 Experimental HOC System

Figure 2 is a schematic of the experimental HOC system implemented to simulate some aspects of an analog photogrammetric instrument. The basic components of this system include a powerful illumination source, the laser; a precise imaging (projection) system; a discriminating sensing system for opto-electronic viewing of selected areas of the double projected images; and an electronic photo diode array detector serving as precise measuring system. Unlike the photogrammetric plotter, a stereomodel is never formed in the HOC. Instead, only one plane parallel to the selected model datum is formed at one time; and the

intersection of that plane with the model surface is determined and designated by the detector array. Before such data are obtained, the proper relative geometry between the overlapping pair of photographs must be accurately recovered as explained in Chapter 2. This will mean the removal of y-parallax at all the model points in the plane for which matching is sought.

When the optical system in the Mach-Zehnder interferometric configuration of the HOC system given in Figure 2 is slightly detuned, a stationary fringe modulation of the superimposed images is created. The fringe spacing should be larger than the detector aperture so that the fringe modulation has a maximum value where the correlation is maximum. Measurement of this fringe modulation is accomplished by translating one mirror (see Figure 1) and simultaneously measuring the time-varying intensity function in the image plane. Detection of the modulated signal at any point in the superimposed output plane forms the basis for the heterodyne optical correlator and effectively increases the signal-to-noise ratio in detection by several orders of magnitude[1].

3.2.1 Experimental HOC Characteristics

The experimental HOC system depicted in Figure 2 contains only one imaging system (L_3 for the detector array, and L_4 for viewing) common to both transparencies instead of one image system for each. This configuration is necessitated by the relative sizes of the illuminated transparencies and the detector array. The illuminating beam has a diameter of about 4 cm at the plane of the transparencies which is reduced by a factor of nominally 5x onto the detector plane. The RETICON photo diode detector array has a matrix of 32 x 32 elements

with an overall size of approximately 3.25 mm x 3.25 mm. Each array element measures 60 μm x 90 μm but the spacing center to center, both horizontally and vertically is 101.6 μm (0.004").

Each transparency is mounted on a carriage which can be translated along any of three mutually orthogonal axes using stepping motors with a least count of 3.175 μm (0.000125 inches). Mechanical mounts were also introduced to allow for the rotation of each transparency about any of its three axes. However, these mounts turned out to pose severe stability problems in the experimental model of HOC and only one rotation in the plane of each transparency was allowed. This obviously changes the photogrammetric basis and further consideration is necessary as will be expounded on in the investigation given in the succeeding section. Suffice it to say here that the two transparencies can be made parallel to each other and to the output (detector) plane to within 5 minutes of arc.

While each transparency can be positioned parallel to the output plane to within 5', each can be reduced onto the array by a somewhat different scale. The determination of that scale is within one digit of the third decimal place in the scale number. Thus for example if the scale is given as 1:6.300, it could be 1:6.299 or 1:6.301 which is a variation of $\pm 1.6 \times 10^{-4}$.

The operation of the experimental HOC is controlled on-line by an HP-21MX mini-computer. The computer sequentially operates the shutters in the two arms of the interferometer to permit selective illumination of the transparencies (i.e. one, the other, or both); it records the necessary array detector data; and computes the normalized correlation coefficient for each detector element.

Other characteristics of the HOC system are:

(1) The spatial resolution of the final imaging system at the plane of the transparency is approximately 20 line pairs/mm.

(2) Given the above spatial resolution, the depth of focus associated with final imaging optics is such that the system can accommodate transparencies with 4% scale differences.

(3) With each array element measuring 60 μm x 90 μm, the correlation area on the transparency is 450 μm x 300 μm.

(4) While one beam path is directed to the detector array, a duplicate beam path permits visual examination of the common image plane with as high a magnification as 100x with a microscope mounted on a three-axis stage for orientation and initialization of the two transparencies.

3.2.2 Investigation of the Effect of Untilting the Transparancies in HOC

We indicated in the preceding section that the introduction of the mounts caused difficulties with regard to the stability of the transparencies. Therefore, the optics specialists indicated that they would much rather have the transparencies untilted in the HOC. This means that within the area on the transparency covered by the array, the aerial photographs are to be assumed as truly vertical. Obviously, due to the existence of tilt, a certain amount of y-parallax will occur within the area of the array. Heterodyne coincidence detection can tolerate some y-parallax with the effect of reducing the value of the maximum normalized correlation coefficient.

In order to quickly ascertain if such an approximation as truly vertical photography within the area covered by the array is plausible, a computational experiment was conducted. A suitable area from a stereopair flown over the Phoenix test range was selected for the experiment. Because the experimental HOC had no accurate means for registration of the transparencies in their holders, a suitable alternative was devised. The projection of two pre-marked corresponding image points are made to coincide in the output plane and used as origin of the coordinate system. The two transparencies are adjusted by rotating each in its plane until no y-parallax exists at <u>two</u> other designated points. This presumes that the value of B_z between the two photographs is insignificant. If this assumption is not valid, then in addition to a rotation in each transparency's plane, a differential projection scale change is also used until y-parallax is eliminated in <u>three</u> image points. The reasoning for this procedure is explained in the following derivation.

For purposes of generality, the plate coordinates of corresponding points are assumed to be referred to the comparator system. The coordinates of the fiducial center are first evaluated

$$x_o = \frac{1}{n} \sum_{i=1}^{n} x_i \qquad y_o = \frac{1}{n} \sum_{i=1}^{n} y_i \tag{4a}$$

$$x'_o = \frac{1}{n} \sum_{i=1}^{n} x'_i \qquad y'_o = \frac{1}{n} \sum_{i=1}^{n} y'_i \tag{4b}$$

where: (x_o, y_o), (x'_o, y'_o) are coordinates of the fiducial centers in the first and second photographs; (x_i, y_i), (x'_i, y'_i) are the coordinates of any fiducial mark in the two photographs,

n is the number of fiducial marks in each photograph.

The fiducial center is used here as the center of coordinates, although in other areas of the model any image point may be used for the purpose as mentioned above.

The coordinates are then shifted to the fiducial centers

$$u = x - x_o \qquad v = y - y_o \tag{5a}$$

$$u' = x' - x'_o \qquad v' = y' - y'_o \tag{5b}$$

where: (u, v), (u', v') are image coordinates on the two photographs, each referred to its fiducial center as origin.

The photographs are placed in the HOC such that when the x-direction of the array passes through the fiducial centers, only x-parallax is made to exist at two points. This is accomplished by having equal y_a coordinates at the two points. Assuming equal scale (i.e. equal magnification between each transparency and the output plane), each photograph will have one rotation angle between its coordinate system and the array system. Consequently, the array coordinates are

$$\begin{bmatrix} x_a \\ y_a \end{bmatrix} = \begin{bmatrix} \cos\alpha & \sin\alpha \\ -\sin\alpha & \cos\alpha \end{bmatrix} \begin{bmatrix} u \\ v \end{bmatrix} \tag{6}$$

from which $$y_a = -u \sin\alpha + v \cos\alpha \tag{7}$$

Applying (7) to two corresponding points on both photographs and equating leads to

$$\begin{aligned} -u_1 \sin\alpha_1 + v_1 \cos\alpha_1 + u'_1 \sin\alpha_2 - v'_1 \cos\alpha_2 &= 0 \\ -u_2 \sin\alpha_1 + v_2 \cos\alpha_2 + u'_2 \sin\alpha_2 - v'_2 \cos\alpha_2 &= 0 \end{aligned} \tag{8}$$

where: the coordinate subscripts refer to the point number, the unprimed coordinates are in one photo and the primed coordinates in the other photo, and α_1 and α_2 are the rotation angles of the first and second photos, respectively (see Figure 3).

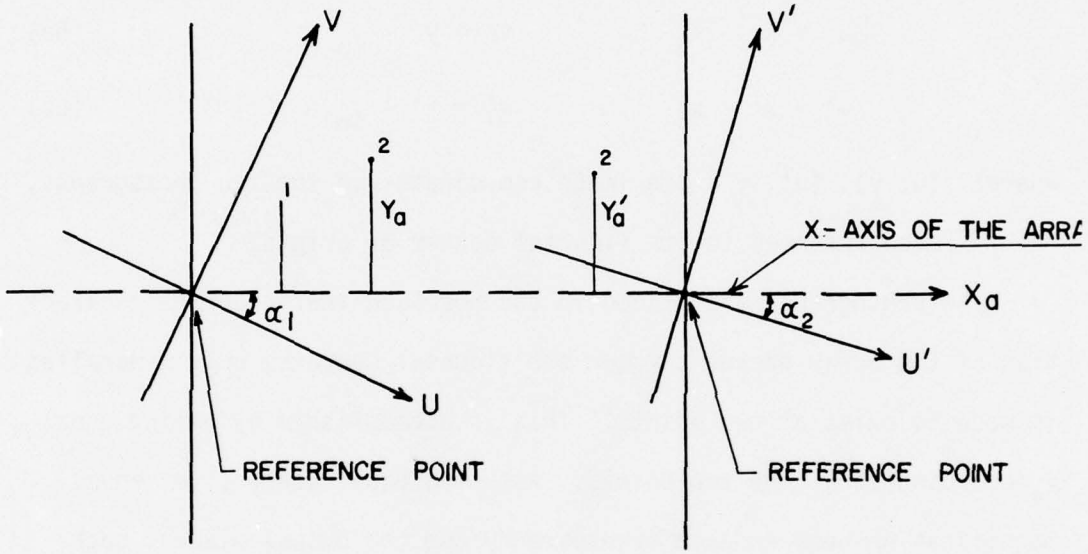

Figure 3. Determination of Zero y-Parallax Direction.

The pair of equations in (8) are non-linear in the unknown angles α_1, α_2. Their linearized form is

$$\begin{bmatrix} (-u_1 \cos \alpha_1^o - v_1 \sin \alpha_1^o) & (u_1' \cos \alpha_2^o + v_1' \sin \alpha_2^o) \\ (-u_2 \cos \alpha_1^o - v_2 \sin \alpha_1^o) & (u_2' \cos \alpha_2^o + v_2' \sin \alpha_2^o \end{bmatrix} \begin{bmatrix} \delta\alpha_1 \\ \delta\alpha_2 \end{bmatrix}$$

$$= \begin{bmatrix} (u_1 \sin \alpha_1^o - v_1 \cos \alpha_1^o - u_1' \sin \alpha_2^o + v_1' \cos \alpha_2') \\ (u_2 \sin \alpha_1^o - v_2 \cos \alpha_1^o - u_2' \sin \alpha_2^o + v_2' \cos \alpha_2') \end{bmatrix} \qquad (9)$$

or

$$\underset{2,2}{C} \quad \underset{2,1}{\Delta} = \underset{2,1}{f} \qquad \Delta = C^{-1} f \qquad (10)$$

The solution from (10) yields corrections $\delta\alpha_1$, $\delta\alpha_2$ to the approximate values α_1^o, α_2^o. The updated values are used again in (9) and the iterative procedure repeated until the corrections are smaller than a preselected tolerance value.

If the value of B_Z is significant, a different scale should be allowed for each transparency as shown in the following derivation.

The y-coordinate with respect to a common x-axis is for the left photograph:

$$y_a = -u \sin \alpha_1 + v \cos \alpha_1 \qquad (11)$$

where: (u, v) are coordinates with respect to either the fiducial center or a reference point in the first photograph,

and for the right photograph:

$$y_a = -au' + bv' \qquad (12)$$

where: $a = s \sin \alpha_2$

$b = s \cos \alpha_2$

s = differential scale between the second and first photographs

(u', v') are the coordinates with respect to the fiducial center in the second photograph.

Equating (11) to (12) and rearranging

$$-u \sin \alpha_1 + v \cos \alpha_1 + au' - bv' = 0 \qquad (13)$$

which contains three unknown parameters α_1, a, and b. Using <u>three</u> points in the overlap area and linearizing

$$\begin{bmatrix} (-u_1 \cos \alpha_1^o - v_1 \sin \alpha_1^o) & u_1' & -v_1' \\ (-u_2 \cos \alpha_1^o - v_2 \sin \alpha_1^o) & u_2' & -v_2' \\ (-u_3 \cos \alpha_1^o - v_3 \sin \alpha_1^o) & u_3' & -v_3' \end{bmatrix} \begin{bmatrix} \delta\alpha_1 \\ \delta a \\ \delta b \end{bmatrix}$$

$$= \begin{bmatrix} (u_1 \sin \alpha_1^o - v_1 \cos \alpha_1^o - a^o u_1' + b^o v_1') \\ (u_2 \sin \alpha_1^o - v_2 \cos \alpha_1^o - a^o u_2' + b^o v_2') \\ (u_3 \sin \alpha_1^o - v_3 \cos \alpha_1^o - a^o u_3' + b^o v_3') \end{bmatrix} \qquad (14)$$

where α_1^o, a^o, b^o are approximate values for the parameters. A suitable set would be $\alpha_1^o = 0$, $a^o = 0$, $b^o = 1.0$. Equation (11) may be written as

$$\underset{3,3}{C} \quad \underset{3,1}{\Delta} = \underset{3,1}{f} \qquad \Delta = C^{-1} f \qquad (15)$$

The solution from (15) gives a correction vector Δ which should be added to the approximate vector and the procedure iterated.

The above procedure was applied to model 98/99 of the Phoenix test area (scale 1:47000). Since for this model the B_z was quite small, only the two parameters α_1 and α_2 were used. In one run, the fiducial center was used as the reference point, that is the origin of the coordinate system. Table 1 gives the y-parallax values and the corresponding u, v, u', v' coordinates for a number of points in the model.

Point No.	y-Parallax (mm)	u (mm)	v (mm)	u' (mm)	v' (mm)
1	.540012E-12	-17.790	-101.483	-103.558	-102.630
2	-.263230	-19.258	-67.137	-104.769	-68.015
3	-.437359	-18.144	-33.457	-103.399	-34.161
4	-.541704	-15.548	1.502	-100.603	.898
5	-.575582	-10.787	35.343	-95.612	35.764
6	-.588942	-16.189	71.462	-100.690	70.912
7	-.508537	-15.980	106.227	-100.115	105.600
8	-.497651	2.393	29.832	-82.732	29.141
9	-.442320	7.900	11.103	-77.349	10.343
10	-.430272	5.335	5.023	-78.967	4.254
11	-.382339	9.938	-6.428	-75.524	-7.255
12	-.283494	16.146	-23.480	-70.147	-24.431
13	-.103798	24.928	-49.044	-61.516	-50.196
14	.125080E-01	19.822	-70.713	-65.909	-71.959
15	.264494	19.334	-104.461	-66.488	-105.958
17	.317256	46.582	-91.771	-40.574	-93.402
20	.255795E-12	45.524	-49.115	-42.369	-50.438
33	-.360915	27.452	67.125	-57.148	66.246
34	-.270274	27.449	107.078	-56.646	106.114

Table 1 Y-Parallax Using Fiducial Center as the Reference Point (Model 98/99 - Phoenix Test Range)

Points #1 and #20 show essentially zero y-parallaxes because they were used as reference for determining the zero-y-parallax direction.

In a second run, point #10 was used as the reference point (i.e. the origin of the uv, u'v' coordinate systems) and points #12 and #24 for the elimination of the y-parallax. Table 2 gives the corresponding values of the y-parallax at a larger set of points than those in Table 1.

Point No.	y-Parallax (mm)	u (mm)	v(mm)	u' (mm)	v'(mm)
12	-.733555E-07	9.811	-28.503	8.820	-28.685
24	-.635779E-07	28.395	-21.534	27.342	-21.836
1	.529316	-24.125	-106.506	-24.591	-106.884
2	.280731	-25.593	-72.150	-25.802	-72.269
3	.112141	-24.479	-38.480	-24.432	-38.415
4	-.112564E-02	-21.883	-3.521	-21.636	-3.356
5	-.476304E-01	-17.122	31.320	-16.645	31.510
6	-.276630E-01	-22.524	66.439	-21.723	66.658
7	.725980E-01	-22.315	101.204	-21.148	101.346
8	-.499056E-01	-3.942	24.809	-3.765	24.887
9	-.148266E-01	1.565	6.080	1.618	6.089
10	0.	0.000	0.000	0.000	0.000
11	.230135E-01	3.603	-11.451	3.443	-11.509
13	.149207	18.593	-54.067	17.451	-54.450
14	.397278	13.487	-75.736	13.058	-76.213
15	.663561	12.999	-109.484	12.479	-110.212
16	.340609	43.659	-103.157	40.660	-104.116
17	.431626	40.247	-96.794	38.393	-97.656
18	.136198	37.531	-79.676	34.815	-80.371
19	-.916821E-01	43.013	-66.056	39.287	-66.718
20	-.155820E-01	39.189	-54.138	36.598	-54.692
21	-.702144E-01	30.775	-47.757	28.204	-48.211
22	-.454529E-01	26.905	-36.981	25.011	-37.344
23	-.197430	17.995	-27.135	15.715	-27.362
25	-.106035	24.118	-18.781	22.459	-19.047
26	-.200315E-01	18.492	-18.740	17.534	-18.954
27	-.528731E-01	7.079	3.358	6.702	3.311
28	-.705945E-01	13.872	11.214	13.424	11.129
29	-.953626E-01	9.176	21.504	8.771	21.468
30	-.174852	13.164	29.611	12.329	29.560
31	-.681945E-01	5.345	33.327	5.425	33.349
32	-.178980E-01	19.575	31.484	19.715	31.386
33	.440020E-01	21.117	62.102	21.819	61.992
34	.169909	21.114	102.055	22.321	101.860
35	-.708802E-01	27.326	13.468	26.697	13.278
36	.662122E-02	34.166	5.830	33.851	5.578
37	-.162407	32.607	2.595	31.055	2.336

Table 2 Y-Parallax Using Point 10 as the Reference Point (Model 98/99 - Phoenix Test Range)

Examination of either Table 1 or Table 2 shows that the y-parallax values are sufficiently large not to be ignored. Consequently, the earlier assumption of tolerable y-parallax within the array area cannot be accepted from the photogrammetric standpoint. If we still wish

to place the transparencies in the HOC without any tilt, another procedure for photogrammetric data extraction must be employed. This is discussed in the following section.

3.3 Operational Mode of the Experimental HOC

If the transparencies are introduced in the HOC such that they are strictly parallel to the output array plane then the data extracted from the HOC become essentially those obtainable from a stereocomparator. This is because the detector array is only a scaled form of the first and fixed photograph and the parallax data, which the moveable transparency yields, can easily be converted into coordinates of the corresponding image points on the second photograph. In this fashion no approximations are made with regard to y-parallax, and the raw HOC data can be rigorously processed to produce the required object space positional information. This apparent change in the basic approach to HOC in no way detracts from its effectiveness as a powerful area correlator capable of parallel processing of a large number of image points.

Because the new HOC operational mode no longer refers to specific contours, a more suitable scheme of data extraction can be implemented. There is no longer a need for shifting the moveable transparency in the x- and y- directions and changing its scale by specific precomputed amounts. Instead, the two transparencies may be projected on the array plane through nominally the same scale (the value of each scale is precisely determined and recorded), and no change in scale is permitted all through the data extraction phase. Once the HOC is initialized at

one point (by effecting coincidence visually or otherwise) the total x- and y- parallaxes, expected to exist within the area covered by the array, are introduced in incremental steps. At each step of say the x-parallax, the moveable transparency is stepped through the entire y-parallax range and a normalized correlation coefficient value at each element in the array is determined. The result of this may be schematically represented in three dimensions as shown in Figure 4. Examination of these values indicates that a maximum value may be determined from the multiple values for each array element. A matrix representing the layout of the array elements may be set up and the number of the step at which the correlation coefficient reached a relative maximum for a given array element is inserted in the corresponding matrix element. This is schematically depicted in Figure 5. In a like manner, stepping is done in the x-direction and a matrix of p_x steps is produced by the processor. The two matrices of p_x and p_y steps are used together with the projection of the array on the fixed photograph to determine the two sets of photo-coordinates of corresponding image points as shown in the following section.

3.3.1 Computation of Ground Coordinates from the Experimental HOC Data

As mentioned earlier, the transparencies are introduced in the HOC and initialized with the help of premarked image points (as opposed to standard fiducial centering as would be the case in a final model of the HOC). Coincidence is established at one image point, and the orientation of the detector array with respect to the fixed transparency, α_1, and the moveable transparency, α_2, determined with the aid of other marked image points. Let x_o, y_o; x'_o, y'_o; i_o, j_o represent the

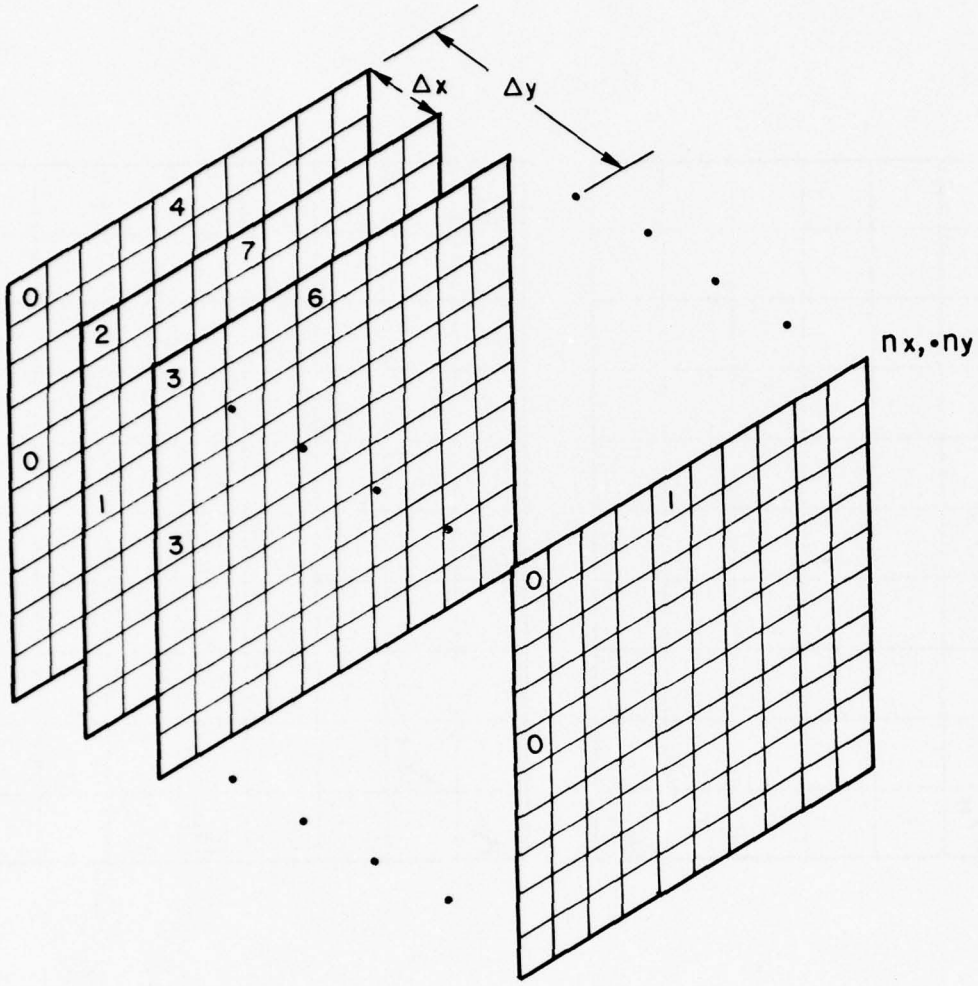

Figure 4. Normalized Correlation Coefficient Values for Several x-Parallax (or y-Parallax) Steps.

Px_{11}	·	·	·	Px_{55}	·	·	·	·	$Px_{10\,10}$
·	Px_{22}								
·		·							
·			·						
Px_{55}				·					
·					·				
·						·			
·							·		
·								·	
$Px_{10\,10}$									·

Py_{11}	·	·	·	Py_{55}	·	·	·	·	$Py_{10\,10}$
·	$Py_{2\,2}$								
·		·							
·			·						
Py_{55}				·					
·					·				
·						·			
·							·		
·								·	
$Py_{10\,10}$									·

Figure 5. The x-parallax (or y-Parallax) Step at which the Normalized Correlation Coefficient Reached a Relative Maximum at Each Array Element.

position of the reference or index point on the stationary transparency, the moveable transparency, and the detector array, respectively. Let, further, r_{x_o} and r_{y_o} be the x- and y- parallax steps at the index point, and k the linear dimension of an array element in the plane of the transparency. If r_x and r_y are the x- and y- parallax steps, respectively, at the ij element, the coordinates of the image point in the stationary transparency is (see Figure 6)

$$\begin{aligned} x &= k(i - i_o) \cos \alpha_1 - k(j - j_o) \sin \alpha_1 + x_o \\ y &= -k(i - i_o) \sin \alpha_1 + k(j - j_o) \cos \alpha_1 + y_o \end{aligned} \tag{16}$$

and on the moveable transparency

$$\begin{aligned} x' = {} & [k(i - i_o) + s_x(r_x - r_{x_o})] \cos \alpha_2 \\ & - [k(j - j_o) + s_y(r_y - r_{y_o})] \sin \alpha_2 + x'_o \\ y' = {} & -[k(i - i_o) + s_x(r_x - r_{x_o})] \sin \alpha_2 \\ & + [k(j - j_o) + s_y(r_y - r_{y_o})] \cos \alpha_2 + y'_o \end{aligned} \tag{17}$$

In equation (17), s_x and s_y are the sizes of the x- and y- parallax steps in the plane of the moveable transparency. If M_1, M_2 are the exterior orientation matrices (object to photo) and f the focal length, then the coordinates on two equivalent truly vertical photographs (assuming positive geometry) are:

$$\begin{bmatrix} u \\ v \\ w \end{bmatrix} = M_1^t \begin{bmatrix} x \\ y \\ -f \end{bmatrix} \quad \text{and} \quad \begin{bmatrix} u' \\ v' \\ w' \end{bmatrix} = M_2^t \begin{bmatrix} x' \\ y' \\ -f \end{bmatrix} \tag{18}$$

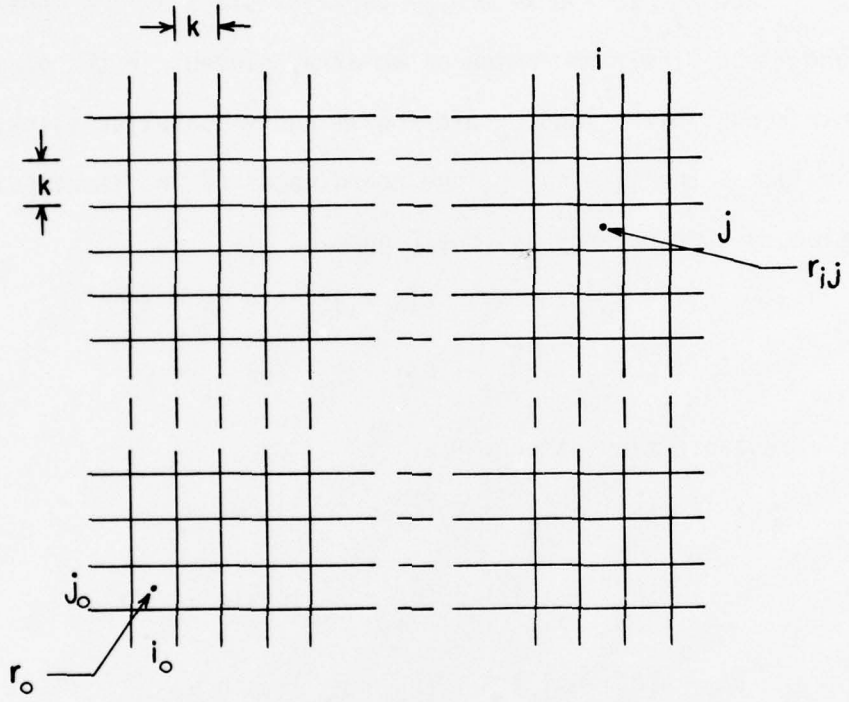

Figure 6. Initialization.

Let X_{c_1}, Y_{c_1}, Z_{c_1} and X_{c_2}, Y_{c_2}, Z_{c_2} be the coordinates (in the object space) of the two camera stations, and X, Y, Z the object coordinates of any point, then

$$\begin{bmatrix} X-X_{c_1} \\ Y-Y_{c_1} \\ Z-Z_{c_1} \end{bmatrix} = t_1 \begin{bmatrix} u \\ v \\ w \end{bmatrix} \quad \text{and} \quad \begin{bmatrix} X-X_{c_2} \\ Y-Y_{c_2} \\ Z-Z_{c_2} \end{bmatrix} = t_2 \begin{bmatrix} u' \\ v' \\ w' \end{bmatrix} \tag{19}$$

where t_1 and t_2 are scale factors, which when eliminated lead to

$$\frac{(X-X_{c_1})}{(Z-Z_{c_1})} = \frac{u}{w} \quad \text{and} \quad \frac{(X-X_{c_2})}{(Z-Z_{c_2})} = \frac{u'}{w'}$$

Then,
$$X = X_{c_1} + \frac{u}{w}(Z-Z_{c_1}) = X_{c_2} + \frac{u'}{w'}(Z-Z_{c_2}) \tag{20}$$

$$Z\left(\frac{u}{w} - \frac{u'}{w'}\right) = \frac{u}{w} Z_{c_1} - \frac{u'}{w'} Z_{c_2} + X_{c_2} - X_{c_1}$$

$$Z \frac{uw' - u'w}{ww'} = \frac{uw' Z_{c_1} - u'w Z_{c_2} + ww' B_X}{ww'}$$

or
$$Z = \frac{uw' Z_{c_1} - u'w Z_{c_2} + ww' B_X}{uw' - u'w} \tag{21}$$

and
$$Y = Y_{c_1} + \frac{v}{w}(Z-Z_{c_1}) = Y_{c_2} + \frac{v'}{w'}(Z-Z_{c_2}) \tag{22}$$

Equations (21), (20) and (22) may be used to compute the elevation and horizontal position for each point in the detector array from the x, y, x', y' coordinates obtained from equations (16) and (17). An alternative procedure which requires more computational effort would be to apply least squares to estimate X, Y, Z from the four collinearity equations obtained from (19) after eliminating the scale factors t_1 and t_2.

3.4 Preliminary Test Results

To investigate the feasibility of the HOC concept aerial transparencies were used on the experimental HOC and the resulting x-parallax values evaluated. It is important to emphasize that the results to follow are both preliminary and limited. They only indicate feasibility and should not be interpreted outside the scope of the experimental nature of the tests. This particular point will be discussed further in the following chapter.

3.4.1 Model 98/99 of the Phoenix Test Range

A subset of the data for the model used in section 3.2.2 was used to obtain the very first data output from HOC. The array was magnified 6.272x onto photo #99 which was stationary. The scale between the array and the moveable photograph, #98, was 6.336. Thus, the area on the transparency covered by the array was approximately 20.5 x 20.5 mm. Point #26 was used as the reference index point, and the direction to point #25 used to establish the x-parallax stepping. Since the y-coordinates of both points #25 and #26 differ relatively little, the rotation from the photo coordinate systems to the array system is adequately represented by

$$\begin{bmatrix} \dot{x} \\ \dot{y} \end{bmatrix} \simeq \begin{bmatrix} 1 & -\delta \\ \delta & 1 \end{bmatrix} \begin{bmatrix} x-x_{26} \\ y-y_{26} \end{bmatrix} \tag{23}$$

where δ is the angle between the coordinate systems in radians. From the comparator plate coordinates the value of δ for each photograph may be computed as:

$$\delta_{99} = \frac{|y_{25} - y_{26}|}{x_{25} - x_{26}} = 0.093/4.925 = 0.018\ 883 \text{ radians}$$

$$\delta_{98} = 0.041/5.626 = 0.007\ 288 \text{ radians}$$

In addition to the two points used in initialization, two other points, #23 and #26 fell within tne array coverage. Figure 7 depicts the HOC output for the x-parallax steps. The few zero values may indicate either lack of sufficient structure for adequate correlation, or that the x-parallax values at these points are outside the stepping range employed.

The index step value at point #26 (position (10, 13) in the matrix) is shown to be 25. Using the original image coordinates and the transformations in equation (23) for each plate the position of points #23, #24, #25 with respect to point #26 were computed and approximately plotted in Figure 7. Then, with coincidence established at point #26, differences in x-parallax were computed and converted to steps (each step is ~ 25 μm, or 0.001 inches). The results are summarized in Table 3.

Point No.	Computed Parallax (mm)	Parallax Step Relative to Point 26
23	1.241	+49.6
24	-0.040	- 1.6
25	0.649	+25.9

Table 3 Check Points for Model 98/99 - Test Range Phoenix

Examination of Figure 7 and Table 3 indicate that these very first results are encouraging. Parallax step for point #23 is 25 + 49.6 = 74.6 which falls in the neighborhood of 71 and 85 in

16 17 20 25 28 30 32 30 62 0 46 83 83 7 5 26 21 20 22 24 22 19 16 15 16 17 19 50 27 36 33 57
14 16 14 77 77 34 37 34 89 53 42 88 44 29 4 25 22 20 29 27 24 21 18 16 15 16 19 19 21 25 25 68
21 21 17 16 28 30 30 0 43 0 53 50 4 34 29 26 23 21 27 29 27 23 20 17 16 15 16 17 19 21 15 29
28 27 21 18 23 24 25 13 26 48 0 43 69 36 33 5 23 23 23 14 30 27 20 18 19 17 16 16 17 20 21 17
35 29 25 20 18 20 23 26 33 0 73 52 87 0 36 32 25 23 25 60 32 25 20 20 23 21 18 17 16 18 21 22
38 33 28 24 22 19 22 24 29 0 83 52 51 56 35 30 27 51 28 82 15 14 23 23 24 21 20 18 16 17 20 22
37 35 32 26 23 20 22 27 0 0 75 51 47 41 37 49 28 11 31 27 33 29 25 23 25 23 21 18 16 17 19 21
36 38 38 33 26 21 21 0 0 0 80 51 52 47 42 27 31 36 32 29 32 32 27 25 25 23 21 20 16 18 18 21
32 40 42 83 30 25 22 79 0 0 45 0 53 45 0 37 35 38 69 31 30 34 29 29 27 25 24 20 17 19 19 20
34 41 44 38 31 28 24 22 79 0 37 0 64 47 45 42 41 40 35 33 79 36 33 31 30 24 21 18 20 20 20 21
4 9 44 39 36 35 30 24 23 43 31 35 46 18 40 0 46 42 40 41 42 40 36 29 26 23 21 19 21 21 20 22
23 68 46 44 42 39 33 29 0 24 40 32 34 34 35 0 0 48 46 45 44 12 78 30 26 24 20 21 23 23 22 23
0 51 44 51 47 45 36 33 30 25 26 28 28 30 0 0 49 51 48 48 41 15 32 30 26 22 20 24 24 26 23 25
47 52 56 57 52 47 39 37 31 28 27 31 32 32 0 0 87 52 47 42 38 65 30 28 23 21 23 24 30 28 25 25
45 52 60 60 55 51 43 40 35 31 28 29 34 37 39 43 10 50 45 42 36 29 26 24 22 22 24 26 31 29 30 28
40 0 81 62 59 53 52 39 37 29 28 30 0 38 54 47 47 47 45 11 36 31 27 22 50 23 25 27 33 34 32 31
39 45 54 62 57 52 44 39 35 31 30 32 35 38 44 44 43 41 39 37 35 32 25 23 25 25 25 29 32 35 37 37
38 44 68 59 57 53 46 38 34 33 31 34 38 41 41 39 37 35 3 25 29 25 24 23 25 25 26 27 34 35 41 43
39 8 84 58 53 48 41 39 37 37 33 33 41 38 37 35 33 31 30 28 26 24 25 26 24 74 25 27 29 31 39 42
42 64 29 57 39 47 43 42 42 41 35 36 40 38 33 31 30 30 28 27 26 25 27 28 28 27 25 25 25 1 34 11
44 89 50 58 55 50 49 0 47 44 39 38 40 35 31 29 29 27 27 27 28 27 28 31 31 31 29 28 26 25 30 34
45 49 53 58 57 57 56 57 40 46 41 41 39 36 31 30 30 30 31 32 31 29 29 33 37 36 35 31 26 26 28 31
41 43 49 63 61 62 62 59 19 51 45 43 41 37 32 31 32 33 9 35 34 31 30 7 87 42 38 36 28 26 26 28
36 43 1 56 52 65 8 65 57 53 24 45 44 5 35 32 30 76 42 41 37 32 31 32 36 44 43 0 31 28 26 26
38 41 47 59 6 11 88 62 71 18 53 51 47 18 38 32 30 36 39 66 42 35 32 4 76 44 46 15 32 30 28 26
40 32 69 55 61 57 71 85 70 71 14 15 11 23 59 30 33 37 43 46 5 15 36 35 51 45 35 39 34 31 28 27
44 47 53 55 65 79 45 41 68 19 44 23 42 52 32 31 8 18 14 63 79 41 40 37 33 71 47 41 39 35 31 28
44 44 41 72 59 55 81 34 59 89 6 63 41 16 36 28 51 1 69 55 78 48 42 40 83 59 49 46 40 37 35 54
47 33 53 35 59 13 32 14 57 54 83 6 45 33 29 47 65 69 53 60 34 0 55 83 44 45 51 50 51 15 76 71
14 81 24 39 26 0 42 20 24 30 56 9 32 34 50 47 39 1 12 56 35 51 76 39 25 30 56 37 32 38 13 25
3 21 3 42 24 37 37 2 52 83 55 7 25 37 58 85 36 64 58 84 25 77 66 89 21 63 55 2 79 88 70 64
10 31 11 28 81 30 32 62 12 73 73 51 20 2 57 30 64 64 50 73 71 81 82 79 85 2 89 69 24 40 69 52

Figure 7. HOC Output for Model 98/99 (x-Parallax).

Figure 7. Similarly, the computed value for point #24 is 25 - 1.6 = 23.4 and falls amongst values of 25, and that for point #25 is 25 + 25.9 = 50.9 and falls at 51. These very preliminary results were sufficiently encouraging to perform another test.

3.4.2 Model 134/135 of the Phoenix Test Range

For this model the original scale plates were not used as in the case of model 98/99 above, but rather the 9" x 9" plates were reduced to 3.25" x 3.25" plates (a factor of ~ 2.77x). Since the main objective of these preliminary tests is to have a feel for how well the HOC correlates, and not how accurate positions may be determined, a special experiment was designed. The center of the area to be covered by the array is marked on both transparencies (which represents the equivalent to a fiducial center). This point was used in the initialization process of the model. Another point closely approximating the y-axis of each transparency was also marked to help in the alignment of the array axis system. In fact, for safety two such auxiliary marks are made, one above and one below the center mark. The coordinates of these three "fiducials" are given in Table 4 for both transparencies.

"Fiducial" No.	Photo 134		Photo 135	
	x (mm)	y (mm)	x (mm)	y (mm)
51	-0.001	14.600	0.003	13.246
52 (center)	0.009	0.000	0.003	0.000
53	0.000	-12.569	-0.003	-12.716

Table 4 "Fiducial" Coordinates for Model 134/135 - Phoenix Test Range

Within the area covered by the detector array, 25 image points were identified, marked, and their coordinates on both transparencies measured using a comparator. The image coordinates are given in Table 5.

	Photo 135		Photo 134	
Pt. No.	x (mm)	y (mm)	x (mm)	y (mm)
1	-3.784	-0.836	-6.439	-0.816
2	-1.046	-2.098	-3.660	-2.090
3	1.108	-2.373	-1.461	-2.368
4	1.371	-5.103	-1.203	-5.107
5	5.922	-4.401	3.485	-4.415
6	9.867	-4.991	7.490	-4.980
7	7.531	-5.951	5.108	-5.960
8	7.441	-10.397	4.971	-10.423
9	2.885	-10.214	0.499	-10.203
10	2.188	0.616	-0.395	0.608
11	1.143	0.435	-1.227	0.449
12	-4.447	1.240	-7.098	1.255
13	-7.977	0.449	-10.649	0.476
14	-7.844	5.160	-10.544	5.174
15	-9.596	7.046	-12.337	7.068
16	-3.653	6.278	-6.312	6.295
17	2.324	6.265	0.104	6.268
18	4.855	6.291	3.271	6.268
19	9.412	6.312	7.848	6.271
20	-2.716	-5.703	-5.185	-5.680
21	-8.640	-5.740	-11.340	-5.704
22	-10.716	-5.707	-13.436	-5.669
23	-10.026	-1.062	-12.730	-1.026
24	-6.753	-1.002	-9.422	-0.978
25	-0.086	6.859	-2.593	6.868

Table 5 Image Point Coordinates for Model 134/135 - Phoenix Test Range

Transparency #135 was introduced in one arm of the HOC and mark #52 centered over element (16, 17) of the array. The array ordinate was made to coincide with the line connecting marks #51 and #52 on the y-axis of transparency #135 which was left stationary. The scale between the array and transparency #135 was 1:6.272. The second and

moveable transparency (#134) was introduced in the second arm and coincidence effected for mark #52. Transparency #134 was also adjusted to align marks #51 and #52 with the vertical array direction. Its scale was 1:6.336.

Since mark #52 did not obviously correspond to an image point, after coincidence was effected, an x-parallax separation of 3.072 mm was introduced. Taking a step of 25 μm in the plane of transparency #134, the step number for any image point may be computed from

$$\text{x-parallax step number} = \frac{1}{0.025}\left[3.072 - \left\{\frac{(x_{135} - 0.003)6.336}{6.272} - x_{134}\right\}\right] \qquad (24)$$

where x_{134} and x_{135} are the x-coordinates of the image point on transparencies 134 and 135, respectively. The quantity between square brackets in equation (24) represents the x-parallax of the point, in millimeter, in the plane of transparency #134.

The coordinates of the 25 points in Table 5 are converted to array elements (using the scale of transparency #135) relative to mark #52, and the results displayed in Table 6. The symbols, L, R, D, U designate left, right, down, up, respectively, with respect to the index point 52 on element (16, 17). Included in Table 6 also are the x-parallax values in millimeters and in terms of parallax steps.

Figure 8 shows the x-parallax step matrix obtained from HOC. The positional data in array element units given in Table 6 were used to approximately plot all the points within the 32 x 32 array in Figure 8.

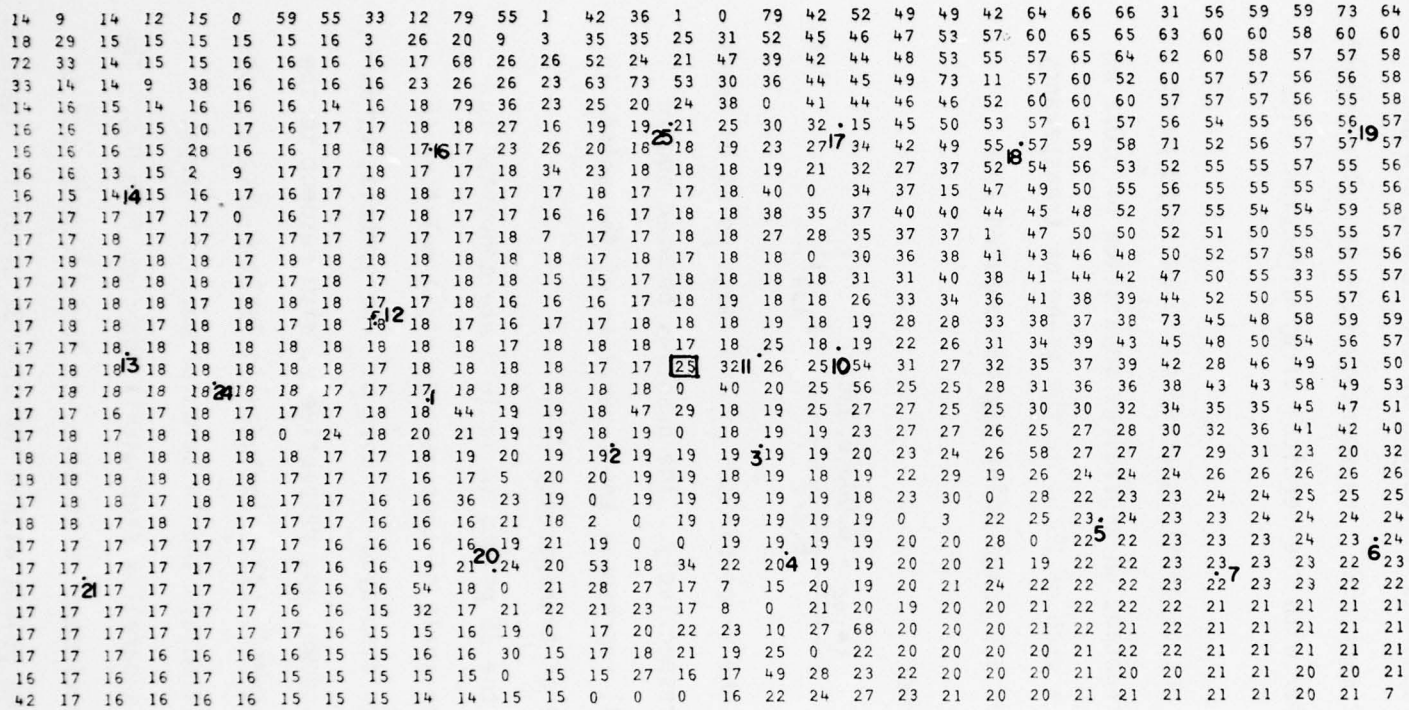

Reference Index Point(16,17)

Figure 8. HOC Output for Model 134/135 (x-Parallax).

Point No.	Array	Position	x-Parallax (mm)	x-Parallax Step
1	L 6	D 1.3	0.459	18.3
2	L 1.7	D 3.4	0.472	18.9
3	R 1.7	D 3.8	0.495	19.8
4	R 2.2	D 8.1	0.487	19.5
5	R 9.4	D 7	0.579	23.
6	R 15.7	D 8	0.597	23.9
7	R 12	D 9.5	0.575	23.
8*	R 11.9	D 16.6	0.529	21.2
9*	R 4.6	D 16.3	0.660	26.4
10	R 3.5	U 1.	0.470	18.8
11	R 1.8	U 0.7	0.693	27.7
12	L 7.1	U 2.	0.469	18.8
13	L 12.7	U 0.7	0.484	19.4
14	L 12.5	U 8.2	0.455	18.2
15*	L 15.3	U 11.2	0.432	17.3
16	L 5.8	U 10.	0.453	18.1
17	R 3.7	U 10.	0.831	33.3
18	R 7.7	U 10.	1.441	57.7
19	R 15.	U 10.1	1.415	56.6
20	L 4.3	D 9.1	0.634	25.3
21	L 13.8	D 9.2	0.463	18.5
22*	L 17.1	D 9.1	0.464	18.5
23*	L 16	D 1.7	0.473	18.9
24	L 10.8	D 1.6	0.475	19.
25	L 0.1	U 10.9	0.569	22.8

Table 6 Check Points for Model 134/135 - Phoenix Test Range

(L = left, R = right, D = down, U = up, relative to (16,17), *points not plotted in Figure 8)

3.4.3 Discussion of Test Results

In the two tests performed, only the x-parallax matrix was extracted from the system because no provision was made in the computer to output the y-parallax matrix. Consequently, the known image data were converted to the HOC output system (instead of the reverse) for purposes of comparison. It is important to note, though, that the stepping in y-direction was properly done in order to eliminate y-parallax and maximize correlation.

Another point worth noting is that the units of comparison are either array element or parallax step. The size of the element in the first test (model 98/99) was about 375 x 570 μm for correlation and 630 x 630 μm for location both at the original 9" x 9" scale. For the second test (model 134/135) the corresponding numbers are 1.04 x 1.58 mm for correlation and 1.75 x 1.75 mm for location. The x-parallax step size used in both tests was 25 μm. Therefore, it becomes apparent that despite having a preliminary experimental system the parallax values came within one to two steps or 25 μm to 50 μm.

CHAPTER 4

CONCLUSIONS AND RECOMMENDATIONS

The Heterodyne Optical Correlator (HOC) is a viable coherent optical system for the simultaneous (parallel) correlation of a large number of sample locations in overlapping imagery. It is unlike most other correlators implemented in automated photogrammetric systems insofar as it is not a tracking correlator. Consequently, the problem of "getting lost" is not relevant to HOC. To be sure, it is similar to other correlators in such aspects as producing false correlation and in the fact that the geometric center of the detector element may not coincide with the density center. But even these problems, are amenable to finding novel and effective solutions due to the nature of HOC.

On the basis of the preliminary results obtained in this report, we can envisage the next system to incorporate the following features:

(1) The original 9" x 9" transparencies may be used directly in HOC

(2) The transparencies may be made parallel to the array plane to within one minute of arc or better

(3) The scale between the array and the transparency may be determined sufficiently accurately to make the effect of any error in its determination on HOC data negligible.

(4) Detector arrays measuring 320 x 512 elements may be used to increase the parallel processing power of HOC, by covering the entire model area at the same time.

(5) The size of the array element will be such that its projection on the transparency is in the range 300 to 500 μm square. Otherwise multiple elements may be used as a unit.

(6) Proper consideration should be given to initialization and indexing of HOC to ascertain that no bias in the output data exists.

(7) Some practical means should be incorporated into the future HOC model for proper visual interaction with the system (e.g. good quality low distortion CRT display accurately connected to the imagery).

(8) The software may consider incorporating corrections for known systematic effects.

Once the above characteristics are implemented, the HOC will offer a good alternative to present correlation systems.

REFERENCES

(1) Balasubramanian, N., "Experimental Heterodyne Optical Correlator (HOC)," U.S. Army Engineer Topographic Laboratories Final Report No. ETL-0071, October 1976.

(2) Mikhail, E. M., "Photogrammetric Analysis of Heterodyne Optical Correlation (HOC) Systems," Report for the Research Institute, U.S. Army Engineer Topographic Laboratories, Contract No. DAAG53-75-C-0184, January, 1976.

(3) Balasubramanian, N., and Leighty, R. D., "Heterodyne Optical Correlation (HOC)," Photogrammetric Engineering and Remote Sensing, December, 1976.